Australas Phys Eng Sci Med (2017) 40:617–629
DOI 10.1007/s13246-017-0571-1

SCIENTIFIC PAPER

Fusion of heart rate variability and pulse rate variability for emotion recognition using lagged poincare plots

Atefeh Goshvarpour[1] · Ataollah Abbasi[1] · Ateke Goshvarpour[1]

Received: 13 March 2017 / Accepted: 4 July 2017 / Published online: 17 July 2017

Abstract Designing an efficient automatic emotion recognition system based on physiological signals has attracted great interests within the research of human–machine interactions. This study was aimed to classify emotional responses by means of a simple dynamic signal processing technique and fusion frameworks. The electrocardiogram and finger pulse activity of 35 participants were recorded during rest condition and when subjects were listening to music intended to stimulate certain emotions. Four emotion categories, including happiness, sadness, peacefulness, and fear were chosen. Estimating heart rate variability (HRV) and pulse rate variability (PRV), 4 Poincare indices in 10 lags were extracted. The support vector machine classifier was used for emotion classification. Both feature level (FL) and decision level (DL) fusion schemes were examined. Significant differences have been observed between lag 1 Poincare plot indices and the other lagged measures. The mean accuracies of 84.1, 82.9, 79.68, and 76.05% were obtained for PRV, DL, FL, and HRV measures, respectively. However, DL outperformed others in discriminating sadness and peacefulness, using SD_1 and total features, correspondingly. In both cases, the classification rates improved up to 92% (with the sensitivity of 95% and specificity of 83.33%). Totally, DL resulted in better performances compared to FL. In addition, the impact of the fusion rules on the classification performances has been confirmed.

Keywords Emotion · Classification · Lagged Poincare plot · Fusion

Introduction

To evaluate cardiac function, various measurements and imaging modalities have been proposed in cardiology. Still electrocardiogram (ECG) and pulse signals are the first choices of the researchers to assess cardiac function. The ECG is a waveform that shows the electrical activity of the heart. It is measured by attaching few electrodes on the limbs or the surface of the chest. ECG has been extensively studied in cardiovascular diseases [1–3] or psychological states such as stress [4] or emotions [5, 6]. A wide range of ECG studies has been conducted using heart rate variability (HRV). The HRV is usually taken from the RR intervals of ECG signals. It demonstrates the balance between vagal and sympathetic heart modulations [7]. Pulse activity recording is performed by fastening piezoelectric sensor to the finger. Finger pulse activity is a simple and low-cost noninvasive technique for monitoring heart rate changes in the peripheral tissues.

Various signal processing techniques have greatly contributed to the research of cardiology. In fact, employing these techniques, subtle features can be extracted which are not available by visual inspection. The majority of human achievements about the cardiac function has come from standard approaches. These techniques were primarily established in the related literature and are still very

✉ Ataollah Abbasi
ata.abbasi@sut.ac.ir
http://ee.sut.ac.ir/Labs/CNLab/index.html

Atefeh Goshvarpour
af_goshvarpour@sut.ac.ir

Ateke Goshvarpour
ak_goshvarpour@sut.ac.ir

[1] Computational Neuroscience Laboratory, Department of Biomedical Engineering, Faculty of Electrical Engineering, Sahand University of Technology, New Sahand Town, P. O. BOX 51335/1996, Tabriz, Iran

common. Time- and frequency- based methods are the two main sub-divisions of standard features. However, cardiac activity is a complex phenomenon which shows nonlinear and chaotic behavior [8]. As a result, nonlinear techniques have attracted many researchers. In addition, different classifications have been proposed to automatically classify psychological states or diseases. Various types of classification methods have been proposed in the previous literature. Each technique has some benefits and shortcomings to deal with classification problems. In this scenario, one of the most challenging topics is emotion recognition.

Emotions play an important role in social interactions, cognition, perception, and generally in daily human life [9, 10], as well as human–machine interactions, such as computer games, online chat, and humanoid robots. Previously, several emotion recognition systems have been suggested based on the physiological signals [11, 12]. In this regard, some efforts have been made to address this problem using cardiac signals [13]. The main goal of this study was to propose an emotion recognition approach based on nonlinear characteristics of ECG and finger pulse activity. In addition, the impact of fusion on the classification rates has been investigated.

Literature review

In this section, the relevant literature with different signal processing approaches and fusion techniques has been reviewed. At the end, we explain our strategy and clarify the differences between our approach and previous studies.

Previous studies on emotion recognition

Previously, several studies have been performed to examine the effect of emotional stimuli on bio-signals characteristics. The first attempt was made using statistical features of five physiological signals [9]. Fisher's projection was applied to classify 8 emotion categories. The maximum accuracy of 81% was reported. Kim et al. [14] examined some linear and spectral features. Using support vector machine (SVM), the maximum rate of 78.4% was achieved for the recognition of 3 emotions. However, the recognition rate reduced to 61.8% for the classification of 4 affective states. Kim and Andre [15] have also attempted to discriminate 4 emotion classes using an emotion-specific multilevel dichotomous classification (EMDC) approach. The system employed different standard and nonlinear features. The maximum recognition rates of 95 and 70% were reported for subject-dependent and subject-independent schemes, respectively. Despite the relatively good results of the EMDC, it cannot be generalized due to a limited number of participants.

The approach in [16] applied wavelet indices of emotional ECG signals. Particle swarm optimization (PSO) and k-nearest neighbor (KNN) were used to classify 2 emotions. The total recognition rate was 84.45%. The approach in [17] applied the normalized statistical features of wavelet coefficients. It was attempted to separate joy, anger, sadness, and pleasure. The authors reported that the proposed technique performed well in discriminating joy and sadness.

Cheuh et al. [18] implemented a statistical technique on the physiological indices to recognize 3 emotions. Six machine learning approaches were evaluated. The results showed the best accuracy of 74.76% using Logistic model. Agrafioti et al. [5] suggested an algorithm based on Hilbert-Huang transform and linear discriminants. The subject-dependent emotion recognition system achieved the highest rate of 89% for the valence dimension. AlZoubi et al. [19] extracted standard features of 3 physiological signals. They examined different machine learning techniques for the automatic detection of the 8 affective states. Using KNN and linear Bayes classifier, the best affect recognition rates were reported. Wavelet based features of HRV were used in [6] to classify disgust, happiness, sadness, fear, and neutral. The maximum accuracy of 88.69% was reached for disgust. Selvaraj et al. [20] attempted to categorize 6 emotions using nonlinear features of the ECG. They implemented Bayesian classifier, regression tree, KNN, and fuzzy KNN. Among them, fuzzy KNN in a subject independent validation scheme resulted in the maximum rate of 76.45%.

Recently, Nardelli et al. [21] attempted to distinguish 4 levels of arousal and 2 levels of valence. They examined various standard and nonlinear HRV features. The classification rates of 84.72% for the valence and 84.26% for the arousal levels were achieved. More recently, a deep-learning methodology was proposed to recognize binary arousal or valence states [22]. The recognition rate was 84%.

In our previous work [23], we applied geometrical analysis of HRV signals to discriminate 4 emotion categories. It has shown that these features can be applied as good markers of emotional responses. The emotion recognition scheme based on geometrical analysis of physiological signals has some advantages; this approach is consistent with the chaotic nature of bio-signals and provides a simple method with low computational load. The effectiveness of this approach has been proven in the literature [21, 24, 25]. Therefore, in the current study, feature extraction was done using Poincare indices.

Previous studies on fusion

In information processing, combining the information from different sources may improve the results. This process is called "fusion". Fusion techniques are generally divided

into a feature based or decision based categories. The former uses the fusion techniques on the original data and on the prior phase of learning. One simple and common manner is to put all features from different modalities into a single vector and fed it into a single classifier. In contrast, the latter implements distinct classifiers. By integrating the results of each classifier, a single decision is shaped.

Fusion is a challenging issue in many sciences and there is no exception for emotion recognition. Emotion recognition based on fusion techniques is still in its infancy. But it is growing rapidly. Many studies have combined the facial modality with biological signals or speech [26–30]. However, a few attempts have been made on the fusion of different bio-signals. Kim and Andre [15] adopted a feature level fusion scheme. They integrated entropy, time–frequency parameters, spectral measures, and geometric indices of 4-channel physiological signals. The highest rates of 95 and 70% were reported for subject-dependent and subject-independent schemes, respectively. By taking the advantages of the speech data and video sequences, Xu et al. [31] proposed an emotion recognition system. A decision level fusion scheme was adopted by two hidden Markov models (HMMs) and artificial neural network (ANN). It was shown that the fusion approach achieved a higher recognition rate than audio- or video- trials.

Verma and Tiwary [32] proposed a multi-modal fusion framework for emotion recognition based on physiological signals. To this effect, 40 channels of bio-signals have been integrated in the system. The average classification rates were 81.45, 74.37, 57.74, and 75.94% for SVM, multilayer perceptron, KNN, and meta multi-class, respectively. Another information fusion approach was adopted based on combining the feature level and decision level fusion techniques [33]. The proposed algorithm classified valence and arousal with the average classification accuracies of 89.24 and 94.06%, respectively. Recently, Lingenfelser et al. [34] included the asynchronous nature of observed modalities in the fusion system. The technique has enhanced the recognition rate by 7.83 and 13.71% compared to video examination and common fusion strategies, respectively. Previously, we proposed a feature level fusion framework to classify emotional states [35, 36]. In this study, both feature level and decision level fusion approaches were examined.

Methods

First, ECG signals and finger pulse waves were recorded simultaneously (Data collection). Then, the heart rate variability (HRV) and pulse rate variability (PRV) were estimated from the successive peak intervals of ECG and finger pulse activity, respectively. After constructing Poincare maps (Poincare plots), some features were extracted as indicators of emotional reactions (Poincare indices). In this study, both feature level and decision level fusion techniques have been examined. The former stacks the features of HRV and PRV together and feeds it into the SVM classifier (Classification). The latter classifies the modalities separately and combines the outputs of the classifiers (Combining classifier). Finally, the results of the decision level fusion technique were compared with the feature level fusion strategy, as well as each SVM classifier individually. The system framework has been demonstrated in Fig. 1.

Data collection

Participants

Finger pulse and ECG signals of 35 college students were recorded while subjects were listening to musical excerpts intended to evoke certain emotions. The participants were 14 females with the mean age of 22.5 ± 1.56 years and 21 males with the mean age of 22.19 ± 1.29 years. All the participants were healthy and no one has reported the cardiovascular, neurological, epileptic, and hypertension disease. They were requested not to use caffeine, salty or fatty foods, 2 h before the test. In addition, they were asked to read a consent form before beginning the experiment, and signed it if they agreed to participate in the trial. The privacy rights of human subjects were always observed and the experiment was conducted in accordance with the ethical principles of the Helsinki Declaration [37].

Emotional stimuli

In the current study, 4 emotion classes, including peacefulness, happiness, sadness, and fear were chosen. 56 short musical excerpts from Vieillard et al. [38] were selected which aimed to induce the emotions. 14 stimuli per each emotional category were presented [38].

KMPlayer was used to play the blocks of music in random order. The subjects were listening to them via headphones at a comfortable volume. The blocks were identical among the participants. The affective stimuli were randomly divided into 12 blocks, and melodies with a similar emotion were inserted in each block. A 6 s of silence was included at the end of each emotional segment.

Data recording

All data were recorded in Computational Neuroscience Laboratory of the Sahand University of Technology. The room temperature and light (laboratory conditions) were kept unchanged for all subjects as far as possible. The mean temperature of the room was about 23 $^{\circ}$C.

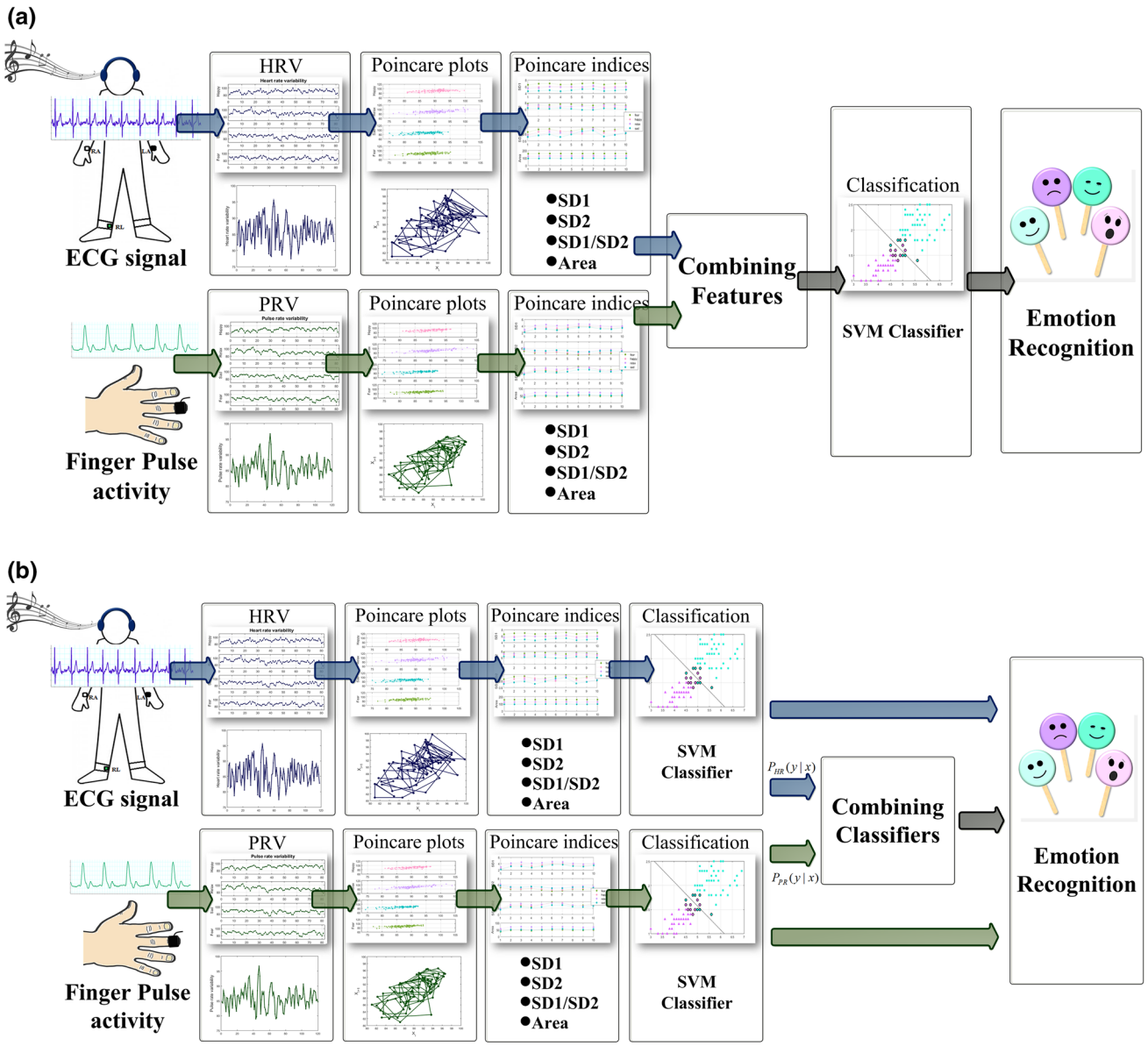

Fig. 1 Outline of the proposed methodology **a** feature level fusion approach and **b** decision level fusion strategy

The participants were asked to lie down in supine position and instructed to remain still during the data acquisition. Initially, the baseline measurement (2 min with eyes closed) was carried out. Then, about 15 min of emotional music were presented.

The finger pulse activity and ECG signals of all participants were collected using 16 channels PowerLab (manufactured by ADInstruments). The beat to beat intervals of both signals were extracted automatically using Chart5 software (ADInstruments, Australia). Then, the time interval between the peaks considered as HRV/PRV for further processing. To remove any artifacts of alternating current line noise, a digital notch filter was adjusted at 50 Hz using Chart5. The sampling rate was 400 Hz. ECGs have been recorded from lead I.

Feature extraction

Lagged poincare plot

Consider HRV time series as X_1, X_2, …, X_N. The Poincare plot is a representation of a time series on a 2D phase space, which plots two consecutive data points (X_i, X_{i+1}). The Poincare plot provides a qualitative visualization. In addition, the dynamics of a time series can be easily understood by means of Poincare plot [39].

Some shape indices are used as quantitative measures of the plot [40]. To this end, an ellipse is fitted on the Poincare plot. The center of the ellipse coincides with the center of the data points. Considering the identity line (a line with unitary slope passing through the origin), two lines pass through the center; longitudinal and transverse lines. They are the major and minor axis of the fitted ellipse and one line is perpendicular to the other. The length of the transverse and longitudinal lines are defined as SD_1 and SD_2, respectively. Therefore, the dispersion of data points along the axis perpendicular to and along with the line of identity is SD_1 and SD_2, correspondingly.

The SD_1 indicates the HRV short-term variability, as well as the parasympathetic activity. In contrast, long-term dynamics of HRV and its overall variability are demonstrated by SD_2. To calculate SD_1 and SD_2, the correlation and mean of the point intervals are determined in lag 0 and lag 1. To control the dependency amongst the variables, a time delay is applied. The SD_1 calculation is performed by (1) and SD_2 is estimated by Eq. (2):

$$SD_1^2 = \gamma_X(0) - \gamma_X(m) \quad \Rightarrow \quad SD_1 = F(\gamma_X(0), \gamma_X(m)) \tag{1}$$

$$SD_2^2 = \gamma_X(0) + \gamma_X(m) - 2\overline{X}^2 \quad \Rightarrow \quad SD_2 = F(\gamma_X(0), \gamma_X(m)) \tag{2}$$

The autocorrelation function for lag m intervals is shown by $\gamma_X(m)$ and the mean value of X intervals is symbolized by $\overline{X}$.

SD_{12} is the ratio between SD_1 and SD_2. It shows the balance between sympathetic/parasympathetic arms or between the short and long X interval variations [40]. It is formulated by (3):

$$SD_{12} = SD_1/SD_2 \tag{3}$$

The area of the ellipse fitted on the Poincare plot [40] is another indicator. It is under the vagal influence and is expressed as (4).

$$S = \pi \times SD_1 \times SD_2 \tag{4}$$

The above mentioned Poincare plot indices were calculated for 10 different lags (1–10).

Classification

SVM was firstly introduced by Cortes and Vapnik [41]. Due to good generalization properties, the SVM was employed as a classifier in this study. It is a supervised classification approach that attempts to classify the points into two different classes. To this end, it finds the optimal hyper-plane, which has the maximum separation margin between the classes.

Consider a data set (T) with i samples:

$$T = \{(x_1, y_1), ..., (x_i, y_i)\}$$
$$i = 1, 2, 3, ..., i \quad x_i \in R^n,\ y_i \in \{\pm 1\} \tag{5}$$

where x_i and y_i represent the inputs and class labels, respectively. The separating line is formulated as follows:

$$\langle w, x\rangle + b = 0 \tag{6}$$

where $w \in R^d$. The inner product of w and x is $\langle w, x\rangle$ and the bias is shown by b. To have the best separating line, the following criteria should be satisfied:

$$(\langle w, x\rangle + b) \geq 1 \tag{7}$$

As the distance from the closest point to the separating line is $\frac{|w^t x_i + b|}{\|w\|} = \frac{1}{\|w\|}$, the margin is equal to $2/\|w\|$. To maximize the margin, $\langle w, w\rangle/2$ should be minimized. As a result, instead of searching for the best separating line, the following optimization criteria should be fulfilled:

$$\min_{w,b} \frac{1}{2}\|w\|^2$$
$$s.t.\ \ z_i(w^t x_i + w_0) \geq 1 \quad \forall i \tag{8}$$

By solving the above equation, the sample set is divided into two groups. Since data is not separated entirely, the SVM uses kernel function and its decision rule is formulated as follows:

$$f(x) = \text{sgn}\left(\sum_{i=1} \alpha_i y_i K(x_i.x) + b\right) \tag{9}$$

where $b = y_i - \sum_{i=1}^{m} y_i \alpha_i (x_i.x_j)$, α_i represents Lagrange multipliers, and $K(x_i, x_j)$ is a kernel function. In the case, the data is projected to a higher dimensional space [41].

In this study, the radial basis function (RBF) kernel was utilized in SVM. In addition, least squares method was used to find the separating hyper-plane.

Decision level fusion

In this study, the Bayesian based theory was applied to fuse the classifiers decision on the HRV and the PRV dynamics.

To predict the class y_m for L classifiers and M classes, the following rules were used [42]:

Rule 1:

$$\arg\ \max_m \frac{1}{L}\sum_{l=1}^{L} P(y_m|\kappa_l) \tag{10}$$

Rule 2:

$$\arg\ \max_m \max_{l=1}^{L} P(y_m|\kappa_l) \tag{11}$$

Rule 3:

$$\arg\ \max_m \underset{l=1}{\overset{L}{med}} P(y_m|\kappa_l) \tag{12}$$

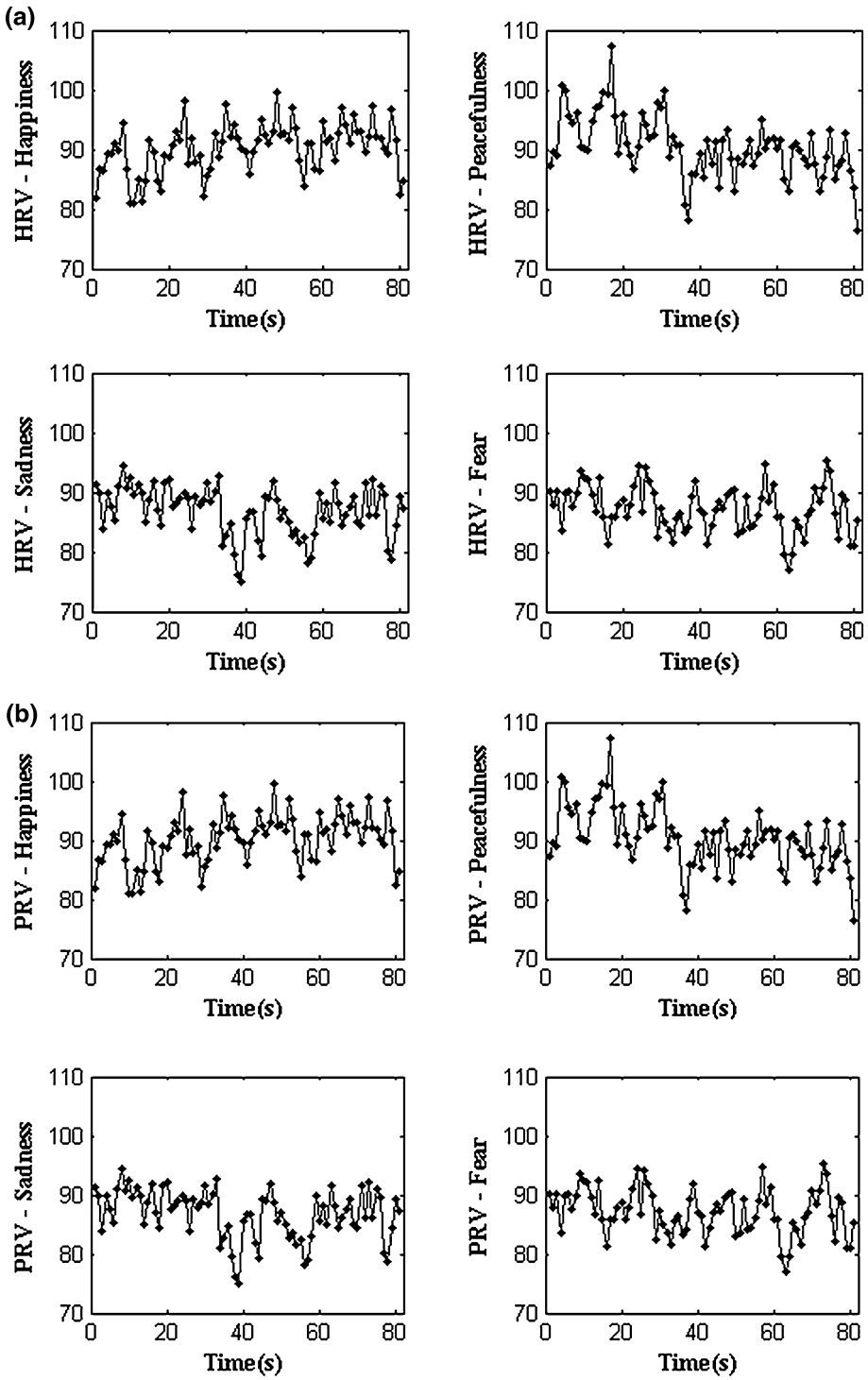

Fig. 2 Estimated **a** HRV, and **b** PRV of a participant in different affective states (subject 5)

Rule 4:

$$\arg \max_{m} \min_{l=1}^{L} P\left(y_m|\kappa_l\right) \tag{13}$$

where κ_l is a classifier and $P\left(y_m|\kappa_l\right)$ is the posteriori probability defined by the sigmoid function for a given future observation x:

$$P\left(y_m|\kappa_l\right) = \frac{1}{1+\exp\left(-y_m f(x)\right)} \tag{14}$$

where $f(x)$ is the result of (9), which indicates the distance between x and the hyper-plane.

In this study, we assumed that $M=2$ and $L=2$. In the case of binary classification problem, the positive class is shown by $y_1=+1$ and the negative one is labeled by $y_2=-1$.

Results

HRV and PRV of all subjects were estimated. Figure 2 shows a typical HRV and PRV.

There are slight morphological differences between HRV and PRV patterns. Then, the Poincare plots with 10 different lags were constructed for both signals during certain emotional states. Figure 3 demonstrates lag 1 Poincare plots o f both signals during rest condition.

To quantify the Poincare plot, 4 indices were extracted from Poincare plot of each signal during emotion elicitation. These indices were also calculated for 10 different lags. The mean values of all Poincare indices were computed for each lag. The results are shown in Fig. 4.

The results (Fig. 4) show that the width and length of trajectories are not the same in different affective states. For HRV signals, the highest mean values of SD_1, SD_2, and area indices are verified in rest condition and happiness (Fig. 4a). As shown in Fig. 4b, higher SD_1 values of PRV are observed in rest condition (top frame). Rest condition, happiness, and sadness have the highest SD_2 values. In contrast, fear and peacefulness have the lowest SD_2 values (bottom frame). Similarly, the highest SD_1/SD_2 and area values are obtained during rest condition. Figure 4 also reveals that the effect of emotional stimuli on the Poincare indices of HRV and PRV is not the same. Considering SD_1 and SD_2, as well as area indices (Fig. 4b), it is obvious that

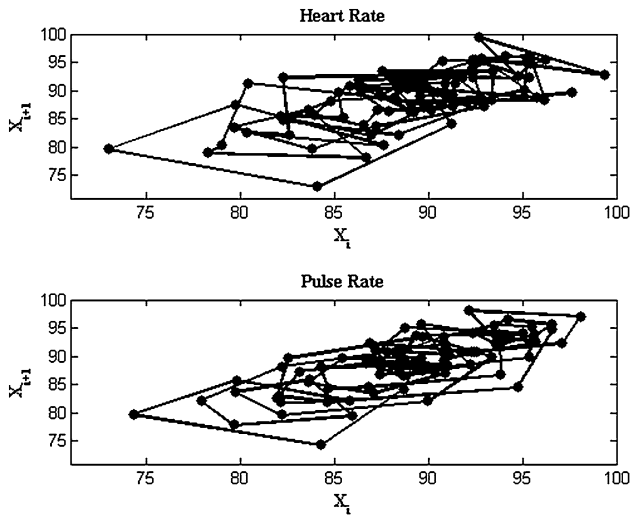

Fig. 3 The Poincare plots in rest condition (subject 5): (*top*) HRV, (*bottom*) PRV

the data points are dense in peacefulness and fear; however, the points are more distributed in the space for rest condition.

To evaluate differences between lagged Poincare measures, the Wilcoxon statistical test was performed. Statistical differences between lag 1 and the other lags are shown in Table 1.

As shown in Table 1, all the Poincare measures show significant differences between lag 1 and the other lags in all states. Smaller p-values are observed for PRV measures, which indicate the reliability of this signal in a typical problem. In addition, the differences are more pronounced between lag 1 and lag 6.

In the next stage, the classifier performances were evaluated by means of accuracy (12), sensitivity (13), and specificity (14).

$$Accuracy = \frac{\text{True Positive} + \text{True Negative}}{\text{True Positive} + \text{True Negative} + \text{False Positive} + \text{False Negative}} \quad (15)$$

$$Sensitivity = \frac{\text{True Positive}}{\text{True Positive} + \text{False Negative}} \quad (16)$$

$$Specificity = \frac{\text{True Negative}}{\text{True Positive} + \text{False Negative}} \quad (17)$$

In addition, two classification strategies were adopted. First, the binary classification results (between rest condition and each affective state) were calculated (BIC). Second, the multiclass classification output was calculated by one vs all (OVA) strategy. In this case, a classifier is trained to distinguish one class from all other classes.

Table 2 shows the BIC classification results for: 1—each HRV/PRV Poincare measure, 2—all HRV/PRV Poincare measures (total features), 3—the combination of features of both modalities as a feature level fusion (FL), and 4—the combination of the classifiers outputs as a decision level fusion (DL) with rule 1. In addition, the OVA classification accuracy has been demonstrated using total features for HRV, PRV, FL, and DL.

Considering each feature separately, the highest BIC classification rates were achieved for separating sadness from rest condition using SD_1. The BIC accuracies were 92, 90, and 88% for DL, HRV, and PRV modalities, respectively. The corresponding sensitivities of 95, 90, and 88.33% were achieved. In addition, the specificities were 93.33, 90, and 93.33%, respectively. The second best BIC results were devoted to fear using SD_1. The BIC classification rates were 92, 88, and 80%, for PRV, DL, and HRV, correspondingly. The sensitivities of 95, 85, and 76.67%, as well as the specificities of 93.33, 100, and 83.33% were obtained.

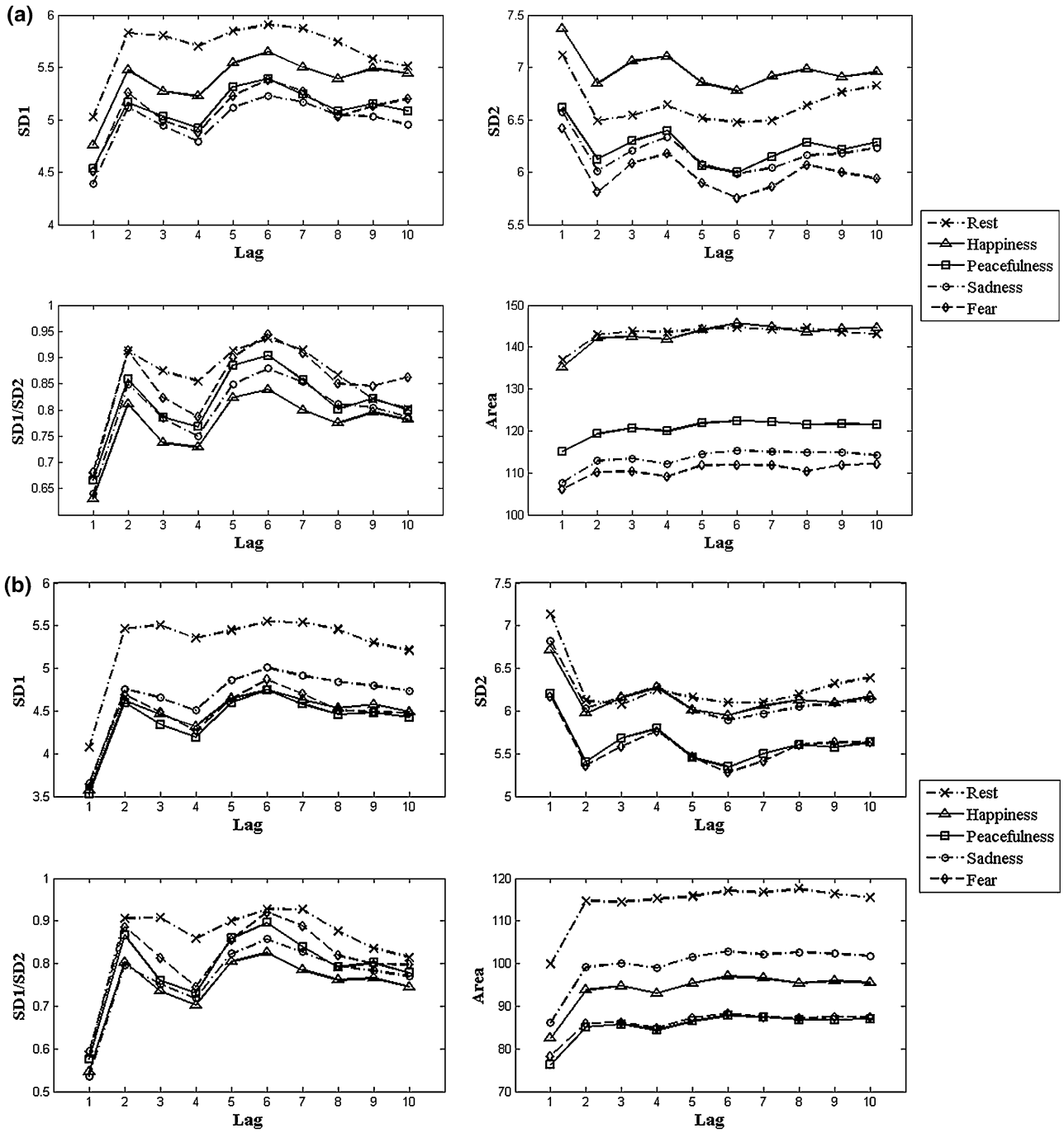

Fig. 4 The mean Poincare plots indices of all participant in different affective states, **a** HRV, and **b** PRV

In terms of features, SD_1 outperformed the other indices with the average BIC accuracy rate of 82.44%. In this case, the mean sensitivity of 86.05% and the average specificity of 83.3% were achieved. The second best BIC classification results were achieved by SD_2. In this case, the mean BIC classification rate was 80% (with the mean sensitivity of 84.19% and the average specificity of 83.4%).

Totally, using PRV, DL, FL, and HRV, the mean BIC accuracies of 84.1, 82.9, 79.68, and 76.05% were achieved, respectively. However, DL technique outperformed the others in discriminating sadness (using SD_1) and peacefulness (using total features) from rest condition. In both cases, the recognition rate of 92%, with the sensitivity of 95% and specificity of 83.33%, was achieved.

Table 1 Statistical test on Poincare measures between lag1 and other lags in different affective states and rest condition

	HRV					PRV				
	Rest	Happiness	Peacefulness	Sadness	Fear	Rest	Happiness	Peacefulness	Sadness	Fear
Lag 1–2										
SD_1	1.40×10^{-7}	3.13×10^{-7}	3.87×10^{-6}	3.32×10^{-7}	3.33×10^{-8}	1.99×10^{-11}	1.38×10^{-11}	9.04×10^{-11}	1.15×10^{-10}	3.98×10^{-9}
SD_2	1.86×10^{-6}	6.88×10^{-6}	2.08×10^{-5}	4.07×10^{-6}	8.50×10^{-7}	1.14×10^{-9}	4.19×10^{-9}	8.31×10^{-9}	2.13×10^{-8}	2.09×10^{-7}
SD_1/SD_2	1.05×10^{-6}	1.09×10^{-6}	1.09×10^{-5}	4.46×10^{-6}	8.74×10^{-6}	6.12×10^{-12}	4.44×10^{-10}	4.15×10^{-9}	2.74×10^{-9}	3.75×10^{-7}
Area	3.47×10^{-4}	0.0017	0.0017	0.0014	0.0031	4.53×10^{-6}	3.03×10^{-6}	1.69×10^{-5}	3.37×10^{-7}	1.04×10^{-5}
Lag 1–3										
SD_1	8.28×10^{-6}	1.02×10^{-4}	2.32×10^{-4}	1.10×10^{-5}	1.13×10^{-4}	4.45×10^{-8}	6.74×10^{-7}	2.18×10^{-6}	1.35×10^{-7}	1.77×10^{-6}
SD_2	1.52×10^{-5}	4.04×10^{-4}	6.09×10^{-4}	2.02×10^{-5}	3.60×10^{-4}	7.69×10^{-7}	6.01×10^{-6}	1.40×10^{-5}	7.71×10^{-7}	1.14×10^{-5}
SD_1/SD_2	4.33×10^{-6}	6.99×10^{-4}	0.0011	6.95×10^{-5}	3.26×10^{-4}	1.74×10^{-8}	4.82×10^{-6}	1.43×10^{-5}	7.93×10^{-8}	2.10×10^{-6}
Area	2.69×10^{-4}	0.0011	1.90×10^{-4}	6.88×10^{-4}	1.67×10^{-4}	9.65×10^{-6}	7.57×10^{-6}	3.26×10^{-6}	1.32×10^{-6}	2.15×10^{-5}
Lag 1–4										
SD_1	2.56×10^{-4}	7.47×10^{-4}	0.0080	0.0097	0.011	1.06×10^{-6}	4.17×10^{-5}	1.3×10^{-4}	4.18×10^{-6}	2.5×10^{-4}
SD_2	4.31×10^{-4}	0.0021	0.028	0.027	0.023	5.43×10^{-6}	2.5×10^{-4}	5.1×10^{-4}	1.41×10^{-5}	6.7×10^{-4}
SD_1/SD_2	9.2×10^{-5}	0.0026	0.017	0.0032	0.015	1.41×10^{-7}	1.3×10^{-4}	5.3×10^{-4}	5.75×10^{-6}	5.2×10^{-4}
Area	8.91×10^{-4}	0.0015	0.0032	0.020	0.040	7.54×10^{-5}	4.99×10^{-5}	1.3×10^{-4}	1.21×10^{-5}	5.6×10^{-4}
Lag 1–5										
SD_1	4.86×10^{-5}	2.80×10^{-8}	2.66×10^{-8}	1.03×10^{-7}	1.41×10^{-7}	5.08×10^{-7}	8.77×10^{-12}	7.08×10^{-10}	1.42×10^{-11}	1.17×10^{-7}
SD_2	7.63×10^{-5}	6.98×10^{-9}	1.41×10^{-8}	3.67×10^{-6}	1.96×10^{-7}	5.73×10^{-7}	8.69×10^{-12}	1.59×10^{-9}	8.90×10^{-11}	6.28×10^{-7}
SD_1/SD_2	1.39×10^{-5}	1.07×10^{-8}	2.47×10^{-7}	4.61×10^{-7}	1.03×10^{-6}	7.85×10^{-8}	3.20×10^{-12}	2.89×10^{-10}	1.85×10^{-11}	1.62×10^{-7}
Area	6.68×10^{-4}	1.13×10^{-4}	5.93×10^{-5}	4.31×10^{-5}	9.17×10^{-6}	2.5×10^{-4}	1.04×10^{-6}	3.20×10^{-6}	9.07×10^{-8}	4.91×10^{-6}
Lag 1–6										
SD_1	1.24×10^{-5}	1.17×10^{-8}	9.28×10^{-8}	1.63×10^{-7}	1.99×10^{-8}	5.23×10^{-9}	5.17×10^{-12}	4.08×10^{-10}	7.96×10^{-12}	2.61×10^{-9}
SD_2	3.04×10^{-5}	4.62×10^{-9}	8.50×10^{-8}	2.23×10^{-7}	1.12×10^{-7}	5.25×10^{-9}	4.78×10^{-12}	1.04×10^{-9}	3.32×10^{-11}	5.07×10^{-8}
SD_1/SD_2	8.80×10^{-8}	9.56×10^{-8}	8.27×10^{-7}	2.42×10^{-7}	1.45×10^{-6}	1.14×10^{-11}	8.88×10^{-12}	3.02×10^{-10}	4.58×10^{-12}	2.06×10^{-9}
Area	2.38×10^{-4}	2.11×10^{-4}	5.65×10^{-5}	3.66×10^{-5}	8.65×10^{-5}	1.56×10^{-5}	1.18×10^{-6}	9.09×10^{-7}	6.47×10^{-8}	2.0×10^{-7}
Lag 1–7										
SD_1	2.21×10^{-6}	1.01×10^{-5}	1.59×10^{-5}	3.67×10^{-6}	1.15×10^{-7}	2.74×10^{-9}	1.14×10^{-7}	3.86×10^{-7}	1.74×10^{-8}	1.86×10^{-7}
SD_2	1.67×10^{-6}	2.31×10^{-5}	2.92×10^{-5}	1.17×10^{-6}	1.61×10^{-7}	1.45×10^{-9}	3.66×10^{-7}	1.47×10^{-6}	2.72×10^{-8}	7.11×10^{-7}
SD_1/SD_2	1.28×10^{-6}	1.58×10^{-5}	3.00×10^{-5}	1.13×10^{-6}	8.21×10^{-6}	3.19×10^{-11}	2.41×10^{-7}	6.41×10^{-7}	1.97×10^{-9}	4.82×10^{-7}
Area	2.79×10^{-4}	7.70×10^{-4}	9.62×10^{-5}	3.07×10^{-4}	7.81×10^{-6}	3.82×10^{-5}	7.25×10^{-6}	2.34×10^{-6}	1.61×10^{-6}	1.35×10^{-5}
Lag 1–8										
SD_1	1.97×10^{-5}	2.43×10^{-5}	1.59×10^{-4}	2.77×10^{-5}	3.56×10^{-4}	1.49×10^{-8}	7.47×10^{-8}	6.09×10^{-7}	3.40×10^{-9}	5.47×10^{-7}
SD_2	5.31×10^{-5}	2.72×10^{-5}	4.47×10^{-4}	3.65×10^{-5}	8.92×10^{-4}	9.52×10^{-9}	1.17×10^{-7}	2.32×10^{-6}	3.42×10^{-9}	2.2×10^{-6}
SD_1/SD_2	4.45×10^{-7}	7.33×10^{-6}	3.70×10^{-4}	7.20×10^{-6}	1.47×10^{-4}	4.93×10^{-11}	2.29×10^{-8}	9.80×10^{-7}	2.85×10^{-10}	1.70×10^{-6}
Area	8.92×10^{-5}	9.09×10^{-4}	1.80×10^{-4}	1.79×10^{-4}	0.0028	2.39×10^{-5}	7.09×10^{-6}	2.69×10^{-6}	2.76×10^{-7}	2.91×10^{-6}

Table 1 (continued)

	HRV					PRV				
	Rest	Happiness	Peacefulness	Sadness	Fear	Rest	Happiness	Peacefulness	Sadness	Fear
Lag 1–9										
SD_1	0.0014	6.68×10^{-8}	2.69×10^{-6}	8.58×10^{-6}	6.60×10^{-7}	1.75×10^{-6}	7.68×10^{-10}	1.16×10^{-8}	1.43×10^{-9}	8.82×10^{-8}
SD_2	0.0042	8.75×10^{-8}	1.55×10^{-6}	1.33×10^{-6}	8.60×10^{-7}	1.98×10^{-6}	1.96×10^{-9}	1.97×10^{-8}	1.21×10^{-9}	1.99×10^{-7}
SD_1/SD_2	1.16×10^{-4}	1.22×10^{-8}	1.27×10^{-6}	4.83×10^{-7}	3.80×10^{-5}	4.46×10^{-8}	4.48×10^{-10}	9.88×10^{-10}	7.61×10^{-12}	5.76×10^{-7}
Area	0.0014	1.42×10^{-4}	1.82×10^{-4}	1.16×10^{-5}	2.87×10^{-6}	1.3×10^{-4}	1.02×10^{-6}	2.81×10^{-6}	3.39×10^{-7}	1.21×10^{-6}
Lag 1–10										
SD_1	0.0031	4.91×10^{-7}	3.39×10^{-5}	1.26×10^{-4}	1.36×10^{-8}	7.11×10^{-6}	1.14×10^{-8}	3.58×10^{-8}	6.59×10^{-9}	6.55×10^{-8}
SD_2	0.013	4.23×10^{-7}	7.12×10^{-5}	2.40×10^{-4}	1.45×10^{-8}	9.55×10^{-6}	3.51×10^{-8}	8.79×10^{-8}	9.38×10^{-9}	1.66×10^{-7}
SD_1/SD_2	2.69×10^{-4}	3.04×10^{-6}	8.30×10^{-5}	3.88×10^{-5}	2.23×10^{-6}	2.34×10^{-7}	7.71×10^{-8}	2.17×10^{-8}	5.10×10^{-10}	1.02×10^{-7}
Area	0.0016	4.81×10^{-4}	2.45×10^{-4}	4.25×10^{-4}	2.99×10^{-6}	3.3×10^{-4}	3.0×10^{-6}	2.31×10^{-6}	5.15×10^{-7}	1.65×10^{-6}

Generally, BIC outperformed the OVA. The highest OVA accuracy of 76.33% was achieved for fear using DL. The second best OVA classification results were obtained for happiness and fear using HRV indices. In this case, the OVA classification rate was 74.67%.

We also evaluated the role of different DL rules on BIC and OVA classification results. Using all features, Table 3 shows the results of different decision level fusion techniques. The best BIC classification rates were achieved using rule 1. The mean BIC accuracy of 82.5% was reached for rule 1. In contrast, the best OVA classification rate was attained using rule 3. However, the mean OVA classification accuracy was nearly 8.5% lower than that of BIC. For different fusion rules, the OVA classification accuracy varied from 70 to 78%. In contrast, using different fusion rules, severe changes have been observed in the BIC accuracies. Therefore, the role of fusion rules on the results has been confirmed.

Discussion

In this study, the nonlinear dynamics of physiological signals have been examined for discrimination of emotional responses. In addition, two fusion strategies have been evaluated using the HRV and PRV modalities. To this end, the bio-signals of 35 subjects were recorded while participants were listening to music. Significant results were attained for PRV. In most cases, improvements in the HRV results have been observed using the FL technique. DL resulted in better performances compared to FL. The results are in the line with previous findings [29]. Using facial expressions and electroencephalography (EEG) modalities for the generation of affective tags, it has shown that DL outperformed the FL.

To construct the feature vectors, lagged Poincare plots (lag 1–10) of 4 emotional states were calculated. Then, 4 geometrical indices were extracted for each lag. The results showed the impact of different affective states on the lagged Poincare indices of both modalities. Rest condition and happiness showed higher SD_1, SD_2, and area values for HRV. For PRV, the highest Poincare measures were obtained during the rest condition. In contrast, lower SD_1, SD_2, and area values were achieved during fear and peacefulness.

Our results also indicated that there are significant differences between lag 1 and other lags in all affective states and rest condition. This finding is in accordance with the previous literature on the affective physiological signals, in which the impact of different lags on the geometry of the Poincare shapes has been proven [23].

Table 2 The classification results for the HRV and PRV measures and two fusion strategies

	SD_1 (%)			SD_2 (%)			SD_1/SD_2 (%)			Area (%)			Total features (%)			
	Ac	Sn	Sp	Ac	Sn	Sp	Ac	Sn	Sp	Ac	Sn	Sp	Ac	Sn	Sp	OVA (Ac)
H																
HRV	80	90	85	72	70	83.33	76	80	90	62	66.67	80	77	87.33	87	74.67
PRV	84	86.67	82	84	86.67	85.33	84	75.02	100	76	81.67	73.33	88	93.33	95	64.67
FL	80.3	81.67	83.33	80	93.4	70	76	76.67	88.33	77.6	93.33	70.03	72	63.44	100	64.62
DL	88	83.33	100	84	83.33	93.33	84	83.33	90	68	76.67	83.33	88	93.33	95	70.67
P																
HRV	72	86.67	60	76	88.33	73.33	72	78.33	70	68	61.67	90	84	83.33	80	68.33
PRV	84	90	76.67	84	90	86.67	80	80	93.34	84	93.33	80	84	95	76.67	67.67
FL	84.4	83.33	90.6	80	88.33	75	76	83.33	70	84	76.67	93.4	84	83.34	93.34	64.62
DL	76	86.67	63.33	76	88.33	73.33	76	80	90	80	78.33	93.33	92	100	80	70.33
S																
HRV	90	90	90	84	86.67	90	76	68.33	86.67	80	81.67	93.33	68	63.33	86.67	66.33
PRV	88	88.33	93.33	84	75.01	100	80	82	88.33	88	88.33	93.33	80	81.67	88.33	72.67
FL	68.4	70.17	75	68	75.33	70	76	93.40	66.87	80	78.33	88.33	68	71.67	68.34	69.23
DL	92	95	93.33	88	86.67	93.33	88	95	88.33	84	86.67	86.67	70	70.01	78.68	71.67
F																
HRV	80	76.67	83.33	72	75	86.67	84	80	93.33	68	78.33	63.33	80	95	84	74.67
PRV	92	95	93.33	80	81.67	86.67	86	90	100	84	88.33	83.33	88	90	92	73
FL	72	88.33	63.60	84	90	80.66	76.40	77.67	83.4	84	81.8	93.3	76	73.34	86.83	61.54
DL	88	85	100	84	88.33	86.67	88	95	95	84	88.33	83.33	80	88.33	85.33	76.33

H happiness, *P* peacefulness, *S* sadness, *F* fear, *Ac* accuracy, *Sn* sensitivity, *Sp* specificity, *FL* feature level fusion, *DL* decision level fusion, *OVA* one vs all

Table 3 The DL classification accuracies for different fusion rules

	Rule 1		Rule 2		Rule 3		Rule 4	
	BIC	OVA	BIC	OVA	BIC	OVA	BIC	OVA
Happiness	88	70.67	80	72.67	68	70.67	76	72.33
Peacefulness	92	70.33	72	74.33	64	75	60	71.34
Sadness	70	71.67	68	69	60	72.33	68	73.67
Fear	80	76.33	64	75	56	78	52	77.33

On the other hand, the nonlinear dynamic properties of autonomic signals have been previously shown [3, 43]. The results of this study confirm the effectiveness of Poincare, as a nonlinear approach, in emotion recognition using physiological signals. These findings are in accordance with the previously published investigations that highlighted the importance of nonlinear analysis in emotion discrimination using bio-signals [21, 44–47].

Affective PRV measures with smaller *p*-values are more likely to be separable than those affective HRV measures with larger *p*-values (Table 1). This was confirmed by the BIC classification performances.

Previously, SVM has been applied in emotion recognition [46, 48, 49]. The results of this study showed higher classification rates than those previously published. Using SVM and empirical mode decomposition (EMD) on ECG, electromyogram, skin conductance, and respiration changes, the correct rate of 76% was reported [48]. In the study conducted by Valenza et al. [46], the spectral, higher order spectral representation, and the Lyapunov exponent of HR signals were fed to the SVM classifier. The average accuracy of 80% was reported. Recently, SVM was applied on the EQ-Radio, a technique for extracting the individual heartbeats from the wireless signal. An average accuracy of 72.3% was achieved in learning person-independent features for emotion recognition [49]. Therefore, the usefulness of the proposed methodology in affect recognition is confirmed.

Conclusion

To sum up, it has shown that nonlinear dynamics of bio-signals can be used to discriminate between affective states and rest condition. The maximum accuracy of 92% was achieved in discriminating both sadness and peacefulness from rest condition. The corresponding sensitivity was 95% and the specificity was 83.33%. Since the best results were achieved for SD_1, the importance of parasympathetic activity in emotion recognition has been proven. On the other hand, we demonstrated that when the information of one modality is not sufficient in a typical classification problem, fusion may be an alternate. Therefore, different bio-signals can offer complementary information.

In conclusion, high classification performances indicate that the proposed approach is promising for automatic emotion recognition. In addition, to improve the classification rates, fusion techniques may be an alternate especially when the information of one modality is not sufficient.

Acknowledgements We gratefully acknowledge Computational Neuroscience Laboratory, where the data were collected and all the subjects volunteered for the study.

Compliance with ethical standards

Conflict of interest The authors declare that they have no conflict of interest.

Ethical approval The privacy rights of human subjects were always observed and the experiment was conducted in accordance with the ethical principles of the Helsinki Declaration.

Informed consent Informed consent was obtained from all individual participants included in the study.

References

1. Moharreri S, Parvaneh S, Dabanloo NJ, Nasrabadi AM (2010) Utilizing occurrence sequence of heart rate's phase space points in order to discriminate heart Arrhythmia. 17th Iranian Conference of Biomedical Engineering (ICBME), IEEE, pp. 1–4
2. Parvaneh S, Hashemi Golpaygani MR, Firoozabadi M, Haghjoo M (2016) Analysis of ECG in phase space for the prediction of spontaneous atrial fibrillation termination. J Electrocardiol 49(6):936–937
3. Tapobrata L, Upendra K, Hrishikesh M, Subrata S, Arunava Das R (2009) Analysis of ECG signal by chaos principle to help automatic diagnosis of myocardial infarction. J Sci Ind Res (JSIR) 68(10):866–870
4. Ghaffari S, Asadzadeh R, Tajlil A, Mohammadalian A, Pourafkari L (2017) Predictive value of exercise stress test–induced ST–segment changes in leads V1 and avR in determining angiographic coronary involvement. Ann Noninvasive Electrocardiol 22(1):e12370
5. Agrafioti F, Hatzinakos D, Anderson AK (2012) ECG pattern analysis for emotion detection. IEEE Trans Affect Comput 3(1):102–115
6. Murugappan M, Murugappan S, Zheng BS (2013) Frequency band analysis of electrocardiogram (ECG) signals for human emotional state classification using discrete wavelet transform (DWT). J Phys Ther Sci 25(7):753–759
7. Camm AJ, Malik M, Bigger JT Jr, Breithardt G, Cerutti S, Cohen RJ, et al (1996) Heart rate variability. Standards of measurement, physiological interpretation, and clinical use. Task Force of the European Society of Cardiology and the North American Society of Pacing and Electrophysiology. Eur Heart J 17(3):354–381
8. Voss A, Schulz S, Schroeder R, Baumert M, Caminal P (2009) Methods derived from nonlinear dynamics for analysing heart rate variability. Philos Trans A Math Phys Eng Sci 367(1887):277–296
9. Picard R, Vyzas E, Healey J (2001) Toward machine emotional intelligence: analysis of affective physiological state. IEEE Trans Pattern Anal Mach Intell 23(10):1175–1191
10. Sander D, Grandjean D, Scherer KR (2005) A systems approach to appraisal mechanisms in emotion. Neural Netw 18(4):317–352
11. Khalili Z, Moradi M (2009) Emotion recognition system using brain and peripheral signals: Using correlation dimension to improve the results of EEG. 2009 International Joint Conference on Neural Networks. Atlanta, pp. 1920–1924
12. Khezri M, Firoozabadi M, Sharafat AR (2015) Reliable emotion recognition system based on dynamic adaptive fusion of forehead biopotentials and physiological signals. Comput Methods Programs Biomed 122(2):149–164
13. Jerritta S, M Murugappan, W Khairunizam, Sazali Y (2014) Electrocardiogram-based emotion recognition system using empirical mode decomposition and discrete Fourier transform. Exp Syst 31(2):110–120
14. Kim K, Bang S, Kim S (2004) Emotion recognition system using short-term monitoring of physiological signals. Med Biol Eng Comput 42(3):419–427
15. Kim J, Andre E (2008) Emotion recognition based on physiological changes in music listening. IEEE Trans Pattern Anal Mach Intell 30(12):2067–2083
16. Defu C, Guangyuan L, Jing C (2009) Toward recognizing two emotion states from ECG signals. 2009 International Conference on Computational Intelligence and Natural Computing, IEEE, Wuhan
17. Long Z, Liu G,.Dai X (2010) Extracting emotional features from ECG by using wavelet transform. 2010 International Conference on Biomedical Engineering and Computer Science (ICBECS), IEEE, Wuhan
18. Chueh TH, Chen TB, Lu HHS, Ju SS, Tao TH, Shaw JH (2012) Statistical prediction of emotional states by physiological signals with MANOVA and machine learning. Intern J Pattern Recognit Artif Intell 26(4):1250008
19. AlZoubi O, D'Mello SK, Calvo RA (2012) Detecting naturalistic expressions of nonbasic affect using physiological signals. IEEE Trans Affect Comput 3(3):298–310
20. Selvaraj J, Murugappan M, Wan K, Yaacob S (2013) Classification of emotional states from electrocardiogram signals: a non-linear approach based on hurst. Biomed Eng Online 12:44
21. Nardelli M, Valenza G, Greco A, Lanata A, Scilingo E (2015) Recognizing emotions induced by affective sounds through heart rate variability. IEEE Trans Affect Comput 6(4):385–394
22. Yin Z, Zhao M, Wang Y, Yang J, Zhang J (2017) Recognition of emotions using multimodal physiological signals and an ensemble deep learning model. Comput Methods Prog Biomed 140:93–110

23. Goshvarpour A, Abbasi A, Goshvarpour A (2017) Indices from lagged Poincare plots of heart rate variability: an efficient nonlinear tool for emotion discrimination. Australas Phys Eng Sci Med. doi:10.1007/s13246-017-0530-x
24. Roque A, Valenti V, Guida H, Campos MF, Knap A, Vanderlei LCM, Ferreira L, Ferreira C, Abreu LD (2013) The effects of auditory stimulation with music on heart rate variability in healthy women. Clinics 68(7):960–967
25. Silva Sd, Guida H, Santos Antonio Ad, Vanderlei LCM, Ferreira LL, de Abreu LC, Sousa F, Valenti V (2014) Auditory stimulation with music influences the geometric indices of heart rate variability in men. Int Arch Med 7:27
26. Busso C, Deng Z, Yildirim S, Bulut M, Lee C, Kazemzadeh A, Lee S, Neumann U, Narayanan S (2004) Analysis of emotion recognition using facial expressions speech and multimodal information. ICMI '04 Proceedings of the 6th international conference on Multimodal interfaces. State College, pp 205–211
27. Go H, Kwak K, Lee D, Chun M (2003) Emotion recognition from facial image and speech signal. Proceeding of the Conference of the Society of Instrument and Control Engineers, Fukui, pp. 2890–2895
28. Wang Y, Guan L (2005) Recognizing human emotion from audiovisual information. IEEE International Conference on Acoustics, Speech, and Signal Processing (ICASSP'05), Philadelphia, pp. 1125–1128
29. Koelstra S, Patras I (2013) Fusion of facial expressions and EEG for implicit affective tagging. Image Vis Comput 31(2):164–174
30. Kachele M, Schels M, Thiam P, Schwenker F (2015) Fusion mappings for multimodal affect recognition. IEEE Symposium Series on Computational Intelligence. IEEE, Cape Town, pp 307–313
31. Xu C, Cao T, Feng Z, Dong C (2012) Multi-Modal Fusion Emotion Recognition Based on HMM and ANN. In: Khachidze V, Wang T, Siddiqui S, Liu V, Cappuccio S, Lim A (eds) Contemporary research on E-business technology and strategy. Communications in Computer and Information Science, vol 332. Springer, Berlin pp. 541–550
32. Verma G, Tiwary U (2014) Multimodal fusion framework: a multiresolution approach for emotion classification and recognition from physiological signals. NeuroImage 102(Pt 1):162–172
33. Naji M, Firoozabadi M, Azadfallah P (2014) A New information fusion approach for recognition of music-induced emotions. IEEE-EMBS International Conference on Biomedical and Health Informatics (BHI), Valencia, pp. 205–208
34. Lingenfelser F, Wagner J, Deng J, Brueckner R, Schuller B, Andre E (2016) Asynchronous and Event-based Fusion Systems for Affect Recognition on Naturalistic Data in Comparison to Conventional Approaches. IEEE Trans Affect Comput PP(99):1
35. Goshvarpour A, Abbasi A, Goshvarpour A, Daneshvar S (2016) Fusion framework for emotional ECG and GSR recognition applying wavelet transform. Iran J Med Phys 13(3):163–173
36. Goshvarpour A, Abbasi A, Goshvarpour A, Daneshvar S (2016) A novel signal-based fusion approach for accurate music emotion recognition. Biomed Eng Appl Basis Commun 28(6):1650040
37. World Medical Association (2013) World medical association declaration of Helsinki: ethical principles for medical research involving human subjects. JAMA 310(20):2191–2194
38. Vieillard S, Peretz I, Gosselin N, Khalfa S, Gagnon L, Bouchard B (2008) Happy, sad, scary and peaceful musical excerpts for research on emotions. Cogn Emot 22(4):720–752
39. Tulppo M, Makikallio T, Takala T, Seppanen T, Huikuri H (1996) Quantitative beat to beat analysis of heart rate dynamics during exercise. Am J Physiol 271(1):H244–H252
40. Guzik P, Piskorski J, Krauze T, Schneider R, Wesseling KH, Wykretowicz A, Wysocki H (2007) Correlations between the Poincare plot and conventional heart rate variability parameters assessed during paced breathing. J Physiol Sci 57(1):63–71
41. Cortes C, Vapnik V (1995) Support-vector networks. Mach Learn 20(3):273–297
42. Kittler J, Hatef M, Duin RPW, Matas J (1998) On combining classifiers. IEEE Trans Pattern Anal Mach Intell 20(3):226–239
43. Wang K, Zhao Y, Sun X, Weng T (2010) A simple way of distinguishing chaotic characteristics in ECG signals. 3rd Int Conf Biomedical Engineering and Informatics (BMEI), IEEE, Yantai, pp 713–716
44. Goshvarpour A, Abbasi A, Goshvarpour A (2015) Affective visual stimuli: Characterization of the picture sequences impacts by means of nonlinear approaches. Basic. Clin Neurosci 6(4):209–222
45. Valenza G, Allegrini P, Lanata A, Scilingo E (2012) Dominant Lyapunov exponent and approximate entropy in heart rate variability during emotional visual elicitation. Front Neuroeng 5:3
46. Valenza G, Citi L, Lanata A, Scilingi E, Barbieri R (2014) Revealing real-time emotional responses: a personalized assessment based on heartbeat dynamics. Sci Rep 4:4998
47. Valenza G, Lanata A, Scilingo E (2012) The role of nonlinear dynamics in affective valence and arousal recognition. IEEE Trans Affect Comput 3(2):237–249
48. Zong C, Chetouani M (2009) Hilbert-Huang transform based physiological signals analysis for emotion recognition. IEEE International Symposium on Signal Processing and Information Technology (ISSPIT), Ajman
49. Zhao M, Adib F, Katabi D (2016) Emotion recognition using wireless signals. Proceedings of the 22nd Annual International Conference on Mobile Computing and Networking (MobiCom '16); New York City, pp. 95–108